Archivum Immunologiae et Therapiae Experimentalis (2019) 67:249–261
https://doi.org/10.1007/s00005-019-00544-7

ORIGINAL ARTICLE

Visfatin Plays a Significant Role in Alleviating Lipopolysaccharide-Induced Apoptosis and Autophagy Through PI3K/AKT Signaling Pathway During Acute Lung Injury in Mice

Xin-Tong Wu[1] · Abdur Rahman Ansari[2] · Xin-Xin Pang[1] · Hui-Zhen Li[1] · Zhe-Wei Zhang[1] · You Luo[1] · Muhammad Arshad[3] · Hui Song[1]

Received: 3 September 2018 / Accepted: 24 April 2019 / Published online: 29 May 2019

Abstract

Visfatin is involved in the body's inflammation and immune response. Inflammation could promote, while visfatin may directly or indirectly mitigate the effects of apoptosis and autophagy. Whether visfatin lessens the detrimental effects of lipopolysaccharide (LPS)-induced mouse acute lung injury (ALI) is poorly understood yet. Therefore, in the current study, the regulation mechanism of visfatin on apoptosis and autophagy was explored in Kunming mice by replicating LPS-induced inflammatory ALI model. Based on the mouse model of ALI, HE staining, TUNEL, transmission electron microscopy, immunohistochemical staining, real-time fluorescence quantitative PCR and western blot were used and the results showed that the alveolar septum was thinner than that of the LPS group, slight lung interstitial and alveolar exudation appeared, and a small number of inflammatory cell infiltration was found in the visfatin intervention group, indicating reduced tissue damage in lungs. After visfatin treatment, the expression of pro-apoptotic genes Bax, Bik, and p53 decreased and the expression of anti-apoptotic genes Bcl-2 and Bcl-xl increased, and expression of autophagy factors LC3 and Beclin1 decreased, indicating that visfatin inhibits apoptosis and reduces autophagy. The expression of PI3K and p-AKT was upregulated in the visfatin intervention group, the expression of AKT was downregulated, and the PI3K/AKT signaling pathway was activated. Hence, visfatin could activate the PI3K/AKT signaling pathway, reduce the apoptotic rate in alveolar epithelial cells and the level of autophagy in ALI by regulating the expression of autophagy factors, ultimately causing a protective effect on lung tissue.

Keywords Visfatin · Acute lung injury · Apoptosis · Autophagy · PI3K/AKT signaling pathway

Introduction

Acute lung injury (ALI) is a critical pulmonary manifestation due to certain inflammatory agents typified by pulmonary oedema and hypoxaemia (Parekh et al. 2011). The acute respiratory distress syndrome (ARDS) is characterized by apoptosis of lung epithelium and impairment of lung tissue barrier functionality (Yen et al. 2013). ALI may lead to inflammatory-induced severe parenchymal damage to lung tissue as well as disruption in integrity of lung epithelium (Chen et al. 2015; Crapo 1986). Lipopolysaccharide (LPS) is a key component of outer double-membrane envelope of Gram-negative bacteria (Okuda et al. 2016; Schwechheimer and Kuehn 2015). Exposure of LPS may induce ALI and ARDS pathogenesis leading to inflammatory reaction (Griet et al. 2014; Yen et al. 2013). Moreover, LPS-induced inflammatory response may cause endotoxemia-mediated ALI in mice (Feng and Jia 2014). Autophagy plays a critical role in inflammatory process and apoptosis in sepsis-induced ALI (Yen et al. 2013). Autophagy and apoptosis are two major processes that determine fat of cells and play critical role in cellular homeostasis, development as well as in a number of physiological and pathological conditions (Mukhopadhyay

✉ Hui Song
songh2007@mail.hzau.edu.cn

1 College of Animal Science and Veterinary Medicine, Huazhong Agricultural University, Wuhan 430070, China

2 Section of Anatomy and Histology, Department of Basic Sciences, College of Veterinary and Animal Sciences (CVAS) Jhang, University of Veterinary and Animal Sciences (UVAS), Lahore, Pakistan

3 Section of Biochemistry, Department of Basic Sciences, College of Veterinary and Animal Sciences (CVAS) Jhang, University of Veterinary and Animal Sciences (UVAS), Lahore, Pakistan

et al. 2014). Several chemicals and therapeutic agents for instance polydatin (Feng and Jia 2014), triterpenoid CDDO-imidazolide (Reddy et al. 2009), carvacrol (Feng and Jia 2014) and angelicin (Liu et al. 2013) have shown anti-inflammatory effects during LPS-induced ALI. Understanding the therapeutic effects of such chemical agents may offer innovative paradigms for establishing significant and novel therapeutic strategies.

Vascular endothelial growth factor (VEGF) plays an essential role in both physiological and pathological angiogenesis (Ferrara et al. 2003). VEGF is a critical pro-angiogenic growth factor, that critically participates in increased vascular permeability and its gene expression is usually regulated by several cytokines (Emani et al. 2009; Pohl-Schickinger et al. 2010). VEGF is a potent as well as powerful direct-acting endothelial permeability mediator that binds to lung vessels and in platelets units in time-dependent fashion (Maloney et al. 2014), implicating a key factor for pulmonary exudate leakage during ALI. Visfatin, a recently discovered adipocytokine (nicotinamide mononucleotide adenylyltransferase or pre-B-cell colony-enhancing factor), is involved in apoptosis, DNA replication and growth regulation as well as repair in several mammalian cells (Bi and Che 2010; Jieyu et al. 2012; Ke et al. 2015). Visfatin is a biochemical as well as genetic marker in ALI that acts as a key factor in mediating several kinds of inflammatory reactions (Sun et al. 2013; Yang et al. 2015). Visfatin acts as an important mediator in the persistence of inflammation and its enhanced levels were detected in ALI, sepsis, inflammatory bowel disease, myocardial infarction and rheumatoid arthritis (Luk et al. 2008). Visfatin plays a critical role in the apoptosis and inflammatory process mediated by the mitochondrial pathway (Xiao et al. 2015). Visfatin also controls the cell apoptosis and inflammation during experimental LPS stimulation (Zhou et al. 2017). Moreover, visfatin treatment notably lessens the necrotic cell death and apoptosis (Erfani et al. 2015). Visfatin acts as a key regulator in the synthesis of LPS-induced inflammatory cytokines in murine macrophages (Wu et al. 2018). Whether visfatin treatment lessens the detrimental effects of LPS on lung tissue through regulating the micro-structure, VEGF expression, apoptosis and autophagy? The aim of current investigation was to explore the regulation mechanism of visfatin on apoptosis and autophagy in LPS-induced inflammatory lung model.

Materials and Methods

Ethics Approval Statement

This study was conducted after the approval from the Animal Care and Use Committee of Huazhong Agricultural University (HZAU), Wuhan, China.

Reagents

We purchased Kunming mice from Hubei Provincial Center for Disease Control, visfatin (PROSPEC, cyt-447-a) from Wuhan Zhong Yi biological reagent, LPS (O111:B4) from Sigma (St. Louis, MO, USA), BCA Protein Quantification Kit from Bi Yuntian Biotechnology Co., Ltd. Shanghai, China, reverse transcription kit and SYBR from TaKaRa, Biomedical Technology (Beijing) Co., Ltd., China, and polyclonal antibody from Cell Signaling Technology, Pudong Shanghai, China.

Test Animals and Treatment

A total of 30 8-week-old, specific pathogen-free (SPF)-grade Kunming mice were purchased from the Hubei Province Disease Control Center (China). They were housed in the Experimental Animal Center of the State Key Laboratory of Huazhong Agricultural University (SPF level). Animals were freely offered to eat and drink, and they were fully acclimated with the environment for 1 week before starting experiments. The experimental animals were randomly divided into three groups based on the similar body weight and the same sex ratio, i.e., the saline group, the LPS group and the visfatin + LPS group. The saline and the LPS groups were intraperitoneally injected with 0.2 ml sterile normal saline daily, and visfatin + LPS group was intraperitoneally injected 0.2 ml of visfatin (100 μg/kg) daily for 7 days. Twelve hours before killing, the normal saline group was injected with 0.2 ml of sterile saline, and both the LPS and the visfatin + LPS groups were injected with 0.2 ml LPS (8 mg/kg). All animals were anesthetized with 1% pentobarbital and killed. The lungs of mice were divided into three parts: one part was fixed in 4% paraformaldehyde and subsequently processed to make paraffin sections; the second part was placed in glutaraldehyde to fix the lung tissues for transmission electron microscopy; the third part of the lung tissue was snap frozen into liquid nitrogen then stored at ultra-low temperature for biomolecular experiments.

HE Staining

HE staining was performed using routinely used protocol. Briefly, the lung tissue sections were stained with hematoxylin for 7 min, treated with 1% hydrochloric acid (HCl) for 1 s and finally stained with eosin for 2 min.

Transmission Electron Microscope

The lung tissues were fixed in 2.5% glutaraldehyde for at least 4 h. The specimen was placed in 1% osmium tetroxide

for 1–2 h and washed three times with 0.1 M phosphate buffered saline (pH 7.4) for 15 min and then kept in 2% aqueous uranyl acetate solution for 30 min. Alcohol dehydration was performed using 50, 70, 90% alcohol, each for 15 min, and finally dehydrated with anhydrous ethanol for 20 min. The specimens were then dehydrated with 100% acetone for 20 min. Anhydrous acetone and embedding agent were mixed in 1:1 ratio by volume and allowed to fully penetrate into the tissue blocks for 2 h, and then in 100% embedding agent for further 2 h. Utrathin (80–100 nm) lung tissue sections were stained with 4% uranium acetate for 20 min, and with lead citrate for 5 min. Electron microscopy was performed using TECNA110 transmission electron microscope.

TUNEL

TUNEL assay was accomplished using the In Situ Cell Apoptosis Detection Kit I, POD (Boster, Wuhan, China). In brief, tissue sections (4 μm) were deparaffinized in xylene, then rehydrated in decreasing concentrations of ethanol. Endogenous peroxidase was blocked in 3% hydrogen peroxide for 10 min and digested in proteinase K for 15 min at 37 °C. The dilution (1:20) of terminal deoxynucleotidyl transferase in a reaction buffer (containing a fixed concentration of digoxigenin-labeled nucleotides) was applied to serial sections for 2 h at 37 °C. The slides were then washed with the stop/wash buffer for 2 min thrice. Following washes, the slide sections were incubated with the prediluted anti-digoxin antibody (dilution 1:100) for 30 min at 37 °C, followed with ABC for 30 min at 37 °C. Apoptotic cells were detected by incubation with the 3,3′-diaminobenzidine chromogen (Boster, Wuhan, China) for approximately 20 min and slides were counterstained with hematoxylin.

Immunohistochemistry

Samples from the lung were fixed in 4% buffered paraformaldehyde solution. After the routine alcohol-xylol process, tissue samples were embedded in paraffin, sectioned at 4–5 μm thickness and stained with HE staining. For immunohistochemistry, primary antibodies of polyclonal light chain 3 (LC3), Beclin1 (Proteintech, Wuhan, China) and the Histostain™ Plus Kit were used (ZSGB Biotechnology, Beijing, China). All immunohistochemical stainings were evaluated by high-power light microscopic examination (BX51; Olympus, Tokyo, Japan).

Real-Time Quantitative Polymerase Chain Reaction

The primers were designed using Primer 3 and the GenBank sequences for GAPDH, Bcl-2, Bax, Bik, Bcl-xl, LC3 and Bclin1 are listed in Table 1. Real-time polymerase chain reaction (RT-PCR; ABI Prism 7000; Applied Biosystems, Beijing, China) was performed to analyze the expression of apoptotic genes using a Fluorescein qPCR Master Mix (×2) (Fermentas China Co., Ltd.). Total RNA was isolated from rat lungs and reverse transcribed to cDNA by a two-step method (Fermentas China Co., Ltd.), followed by real-time quantitative PCR (RT-qPCR). Briefly, 10 μl of master mix, 0.8 μl of primer assay (×10) and 4 μl of template cDNA (×10) were added to each well. After centrifugation, the parameters used for PCR reactions were as follows: PCR activation at one cycle of 50 °C for 2 min, 95 °C for 5 min, followed by 40 cycles of 95 °C for 30 s and 60 °C for 30 s. All samples and controls were run in triplicates on an ABI 7000 Fast RT-PCR system. The RT-qPCR data were analyzed by a comparative threshold (CT) method. The results were expressed as the ratio of reference gene to target gene using the following formula: CT = CT (target genes) − CT (GAPDH). To determine the relative expression levels, the following formula was used: CT = CT (treated group) − CT (saline group). Thus, mRNA levels were normalized to those of GAPDH. Relative mRNA levels are shown using arbitrary units and the value of the saline group is defined as one.

Western Blot

Frozen lung tissue preparations were homogenized with sample buffer, centrifuged and boiled. Total protein concentration of the lung tissue was quantified using the Bradford method. Protein concentrations were determined using the BioRad protein assay (Bio-Rad, Hercules, CA, USA). Equal amounts of total protein were loaded onto 1% SDS-PAGE and then electrophoretically transferred onto polyvinylidene difluoride membranes (IPVH00010; Millipore, Beijing, China). Transferred membranes were blocked using

Table 1 Primers used for RT-qPCR

Gene name	Forward primer (5′→3′)	Reverse primer (5′→3′)
GAPDH	TGCGACTTCAACAGCAACTC	TCCCCACATACCAGAAAGT
LC3	TTCTTCCTCCTGGTGAATGG	ATTGCTGTCCCGAATGTCTC
Beclin1	TCTGGAAGATGGGTCTGTGA	GTGTAGGCGGGGTTGTTATG
Bax	CGTGAGCGGCTGCTTGTCTG	ATGGTGAGCGAGGCGGTGAG
Bik	ACAGCCGGACAGGTGTCAGAG	CCAGCAGCAAGAAGACCAGCAG
Bcl-2	TCCTTCCAGCCTGAGAGCAACC	TCACGACGGTAGCGACGAGAG
Bcl-xl	AACAATGCAGCAGCCGAGAGC	GCAGAACCACACCAGCCACAG

5% skim milk and incubated overnight with antibodies p53, MLKL, LC3, Beclin1, PI3K, AKT (Proteintech, Wuhan, China) and p-AKT(CST). The same membrane was probed with anti-GAPDH (ABclonal, Biological Technology Co., Ltd. Wuhan, China) as house-keeping protein. After washing with TBST three times, the blots were hybridized with secondary antibodies (1:50,000 dilution; Boster, Wuhan, China) conjugated with horseradish peroxidase for 2 h at room temperature. The antibody-specific protein was visualized by enhanced chemiluminescence detection system.

Statistical Analysis

Statistical analysis was performed using the Statistical Package for the Social Sciences (SPSS, v.17.0; SPSS, Chicago, IL, USA) and Graphpad Prism 5 software (Graphpad, San Diego, CA, USA). The ANOVA test was used for comparisons between groups. Differences were considered statistically significant at P values of ≤ 0.05. All data were expressed as mean $\pm$ SD.

Results

Structural Changes of Lung Tissue in Different Experimental Groups

Histopathological Alterations in Mouse Lung Tissue

The results of HE staining showed that the structure of lung tissue in the saline control group was clear and complete, the alveolar wall was thin, and there was no effusion in the alveoli and no inflammatory cell infiltration. ALI model group (LPS group) showed obvious lung injury, significantly thickening in alveolar wall, enhanced inflammatory cell infiltration, along with considerable pulmonary interstitial and alveolar hemorrhage. LPS + visfatin group illustrated lessened lung injury, somewhat thicker alveolar septum, slight alveolar hyperemia, very minute pulmonary interstitial and alveolar exudation and a little inflammatory cell infiltration than the control group (Fig. 1a–c).

VEGF Expression Changes in Mouse Lung Tissue

Immunohistochemistry results showed a little or no VEGF expression in alveolar epithelial cells and bronchial epithelial cells in saline control group. The expression of VEGF was increased, the pulmonary alveolar neutrophil and monocyte were seen in the nodular inflamed cells, and alveolar as well as bronchial epithelial cells were significantly enhanced in the lung tissue of ALI model group (LPS group).

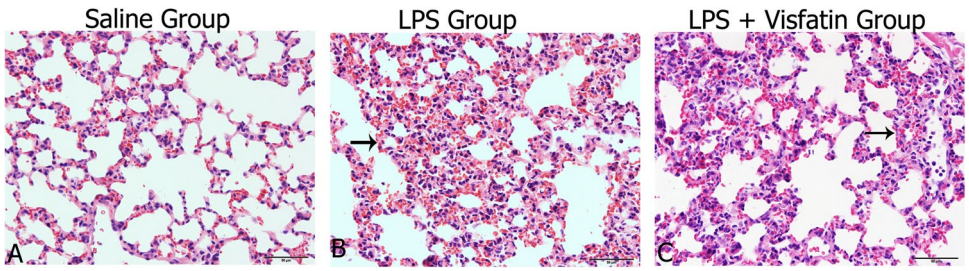

Fig. 1 The changes in histological structure of mouse lung tissues (×40) in different groups. The black arrow indicates the alveolar septum thickening, the purple staining dot indicates inflammatory cells, and the red staining dot indicates red blood cells. Where in-figure letter, **a** saline group; **b** LPS group; **c** LPS + visfatin group

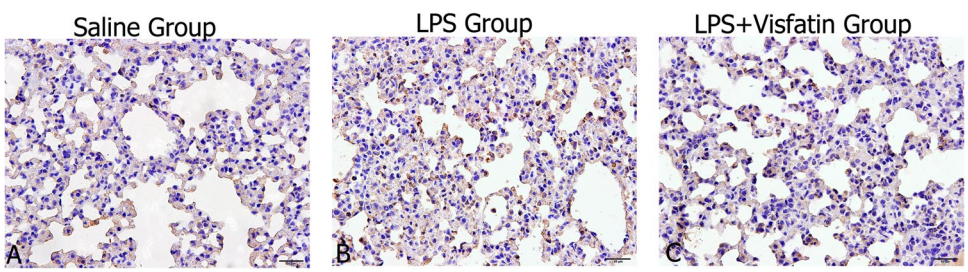

Fig. 2 The expression of VEGF in different groups of mouse lung tissues. Yellowish brown reaction product refers to VEGF-positive signal distribution. Where in-figure letter, **a** saline group; **b** LPS group; **c** Visfatin + LPS group

LPS + visfatin group showed significantly reduced lung tissue VEGF expression compared to LPS group (Fig. 2a–c).

Effect of Visfatin on Apoptosis of Lung Tissue in ALI

Detection of Apoptotic Cells

TUNEL method was used to detect the apoptosis of mice lung tissue that appeared as brownish yellow cells in each group. The apoptotic cells were mainly distributed in alveolar and bronchial epithelial cells. The saline control group had fewer apoptotic cells in the lung tissue. The number of apoptotic cells in LPS group significantly increased. The number of apoptotic cells in LPS + visfatin group significantly decreased compared with LPS group (Fig. 3a–c). To determine the experimental results quantitatively, the image pro plus (IPP) software was used to calculate the average optical density (IOD) value of apoptotic cells in each group of mice. The results showed that IOD of LPS group was significantly increased ($P < 0.01$) compared to the saline control group. However, LPS + visfatin group showed significantly lower IOD values as calculated by IPP than that of LPS group ($P < 0.05$) (Fig. 3d).

The mRNA Expression of Apoptotic Factors in Different Experimental Groups

The Bcl-2 gene family includes the anti-apoptotic factors, such as Bcl-2, Bcl-xl, Bcl-w, Mcl-1, Nr13, and the pro-apoptotic factors, such as Bax, Bik, Bak, Bad, Bid and so on. The results of RT-qPCR showed that the expressions of Bax and Bik were significantly increased ($P < 0.01$, $P < 0.05$) in LPS group compared to the saline control group. The mRNA expressions of anti-apoptotic factors Bcl-2 and Bcl-xl were significant increased ($P < 0.01$) in LPS + visfatin group compared with LPS group (Fig. 4a–e).

The Protein Expression of Apoptosis-Related Factors in Different Experimental Groups

The expression of apoptosis-related protein P53, a tumor suppressor gene, can promote apoptosis while MLKL gene regulates necrotic apoptosis. Western blot results showed that, compared with saline control group, P53 and MLKL protein expression were significantly increased in LPS group. Compared with the LPS group, the protein expression of P53 and MLKL in LPS + visfatin group showed a decreasing trend (Fig. 5a, c). ImageJ software was used to quantify the gray value of P53 and MLKL in western blot. The statistical results showed that, compared with the saline control group, P53 and MLKL gray values increased significantly in LPS group. Compared with LPS group, the gray values of P53 and MLKL decreased in LPS + visfatin group (Fig. 5b, d).

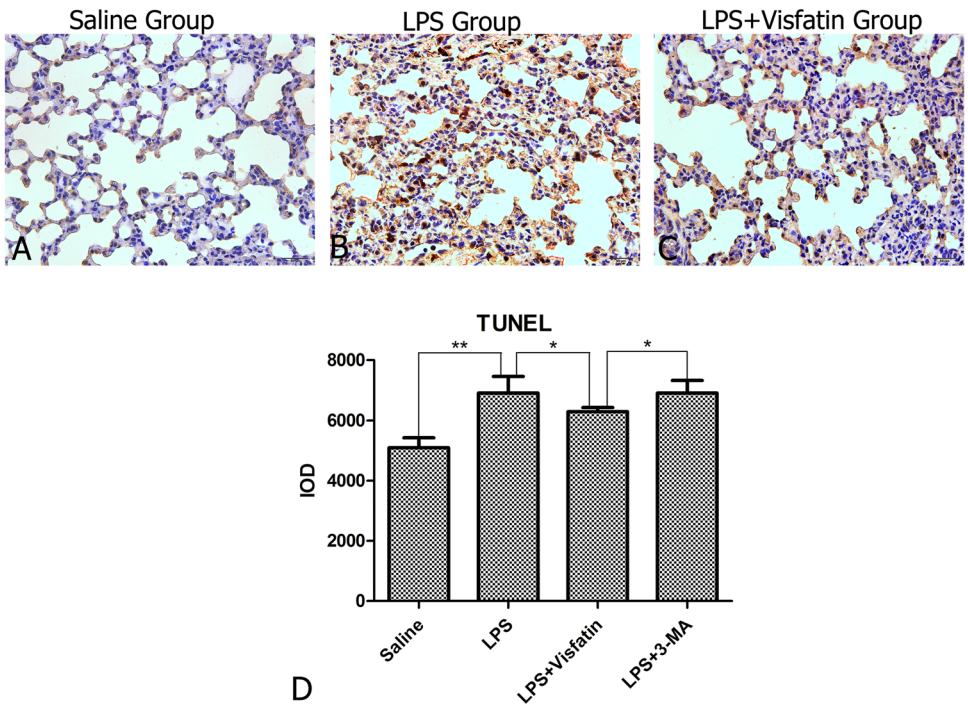

Fig. 3 The changes of apoptosis in different groups of lung tissues. Yellowish brown reaction product refers to apoptosis cell positive signal distribution (**a**–**c**). The detection of apoptosis-positive cells IOD values (**d**). Where in-figure letter, **a** saline group; **b** LPS group; **c** LPS + visfatin group; **d** IOD value graph. *$P < 0.05$ and **$P < 0.01$

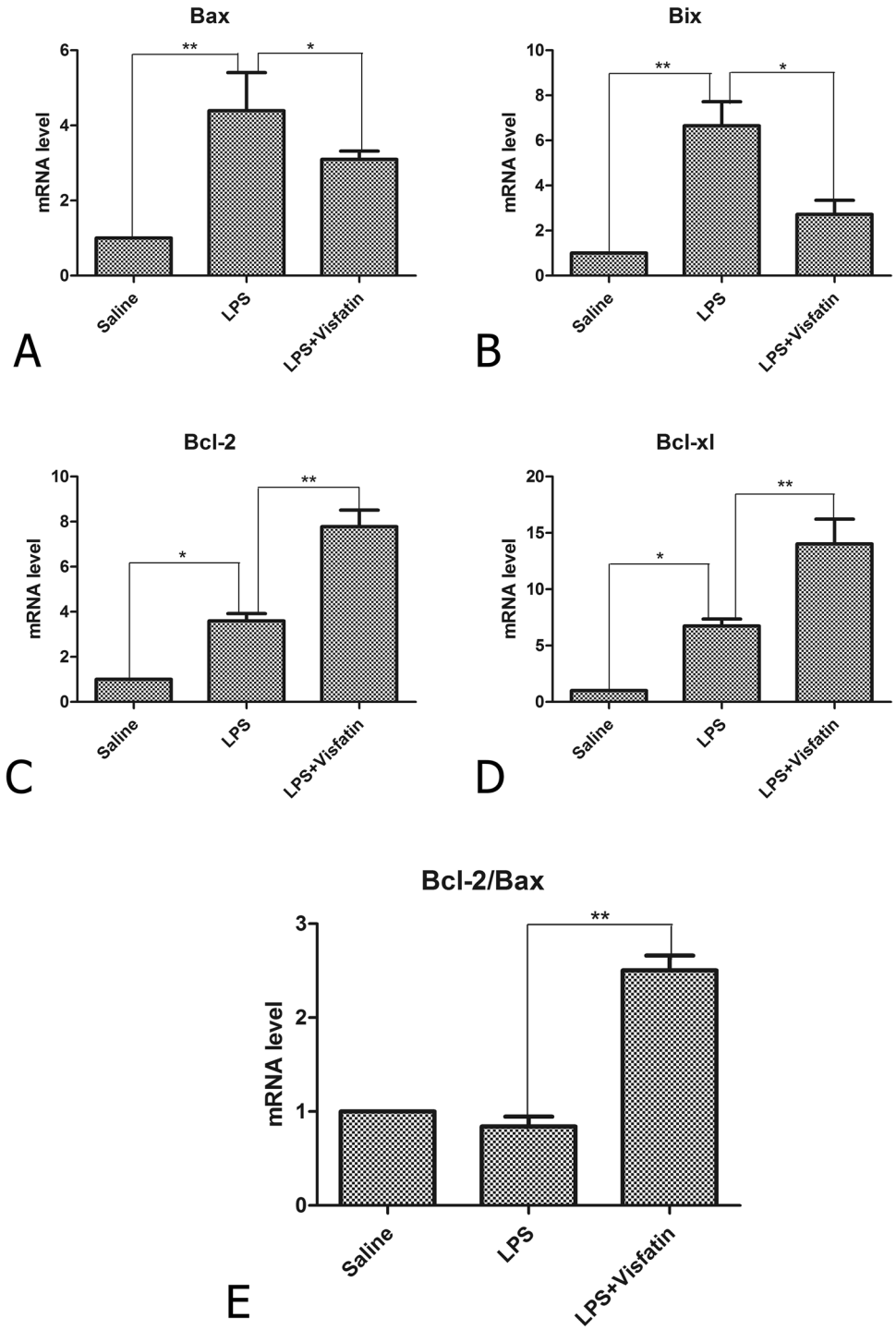

Fig. 4 The mRNA expression level of apoptosis factors in different groups of lung tissues. The mRNA expression of apoptotic factors in lung tissue was analyzed in each group by one-way ANOVA using SPSS software and Graph Pad Prism 5 software (**a**–**d**). In addition, the Bcl-2/Bax ratio was calculated (**e**). $^{*}P < 0.05$, $^{**}P < 0.01$

Effect of Visfatin on Autophagy in Lung Cells of ALI

Transmission Electron Microscopy was Used to Detect Autophagosomes

Transmission electron microscopy can intuitively observe autophagosomes. Autophagosomes are hallmark of autophagy. The results showed that there were a few autophagosomes in the saline control group, the number of autophagy bodies in the LPS group was significantly increased, and mitochondria were swollen. Compared with LPS group, the number of autophagosomes in LPS + visfatin group significantly reduced, but slightly more than that of the saline control group (Fig. 6a–c).

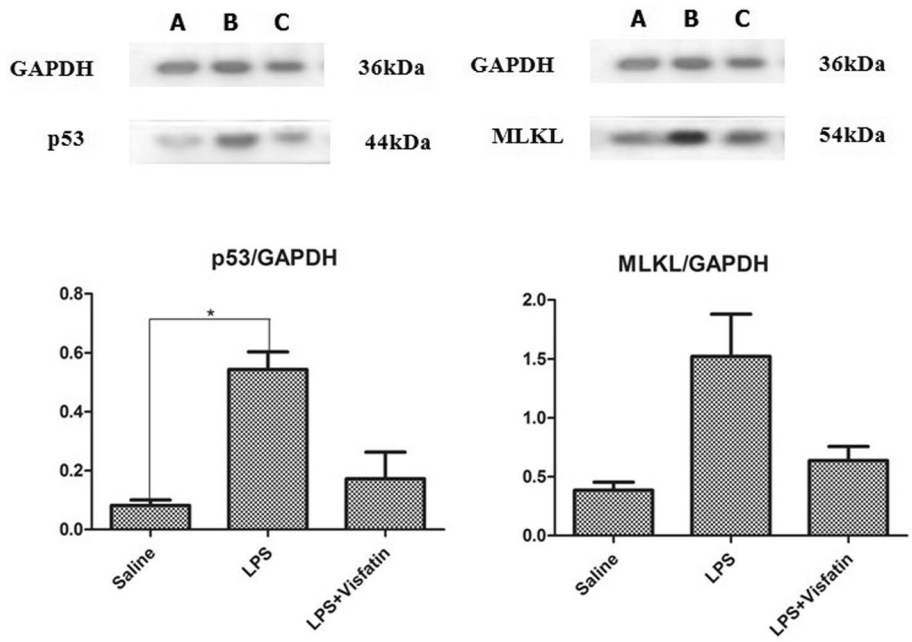

Fig. 5 Western blots of total p53, MLKL and their gray values. The western blots of p53 and MLKL with relative expression of GAPDH. Where in-figure letter, A: saline group; B: LPS group; C: LPS + Visfatin group

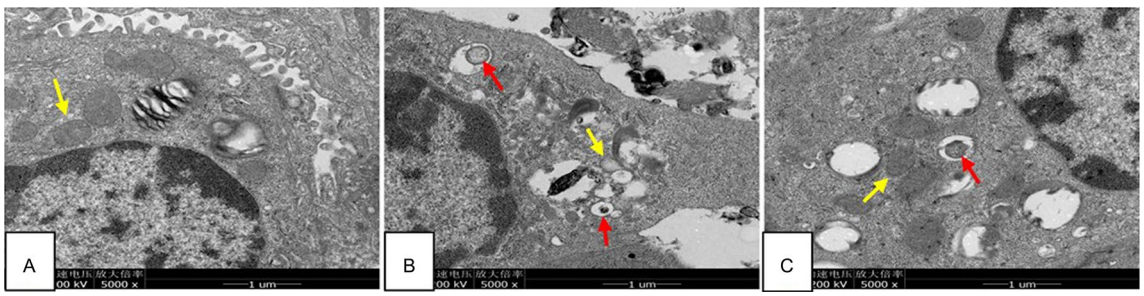

Fig. 6 Changes of autophagosomes in different groups of lung tissues. The electron micrographs show alterations in autophagy. Red arrows refer to autophagosomes; yellow arrows refer to mitochondria (**a**–**c**). Where in-figure letter, **a** saline group; **b** LPS group; **c** LPS + visfatin group

Localization and Expression of Autophagy Factors in Different Experimental Groups

LC3 and Beclin1 are important factors for testing autophagy. Immunohistochemical results showed that the brownish yellow positive products were present in bronchial epithelial, vascular endothelial and alveolar epithelial cells. LC3 was largely expressed in the cytoplasm, particularly in the alveolar septal epithelial cells. LC3 expression was significantly increased in the LPS group compared with the saline control group. The expression of LC3 decreased in LPS + visfatin group compared to LPS group (Fig. 7a–c). The average IOD values of immunohistochemical positive products of LC3 expression were semi-quantitatively studied by IPP software. The statistical results showed that, compared with the saline control group, LC3 expression was significantly increased ($P < 0.01$) in LPS group, while compared with LPS group LC3 expression was significantly decreased ($P < 0.01$) in LPS + visfatin group (Fig. 7d).

Similarly, immunohistochemical results showed that the brownish yellow positive products of Beclin1 were mainly expressed in alveolar epithelial and in nodular inflamed cells. Beclin1 expression was significantly increased in the LPS group compared with the saline control group. The expression of Beclin1 decreased in LPS + visfatin group compared to LPS group (Fig. 8a–c). The average IOD values of Beclin1 expression showed that, compared with the saline control group, Beclin1 expression was significantly increased ($P < 0.01$) in LPS group, while compared with LPS group Beclin1 expression was significantly decreased ($P < 0.01$) in LPS + visfatin group (Fig. 8d).

mRNA and Protein Expression Changes in Autophagy

Quantitative PCR was used to detect the mRNA expression of autophagic factors LC3 and Beclin1. The results showed that the mRNA expression of both LC3 and Beclin1 was lower in the saline control group but relatively

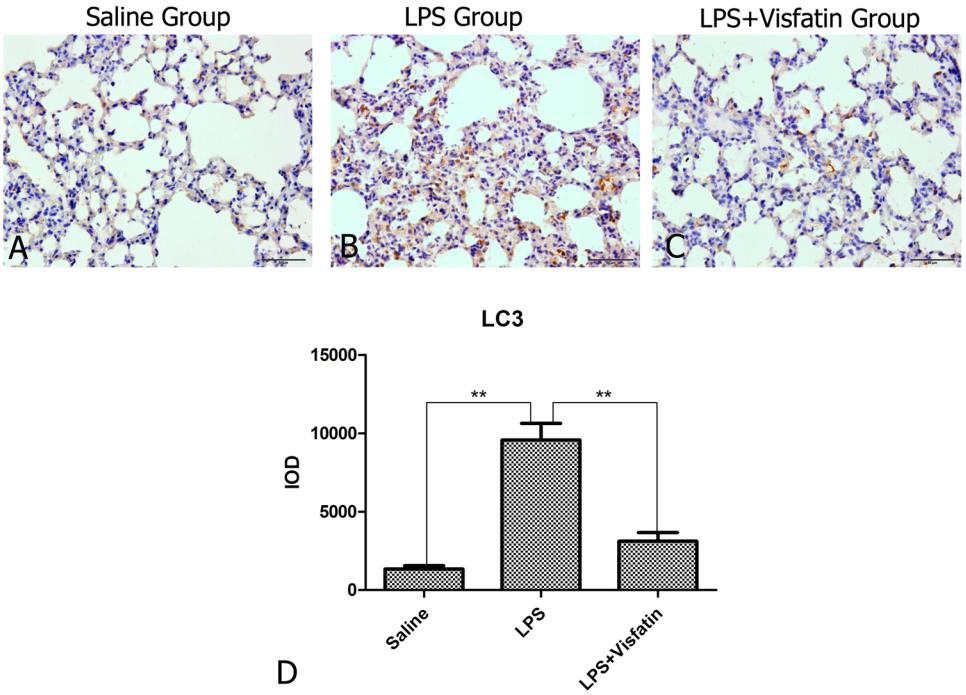

Fig. 7 The distribution pattern of LC3 expression in different groups of lung tissues (immunohistochemistry). Yellowish brown reaction product refers to LC3 protein-positive signal distribution (**a**–**c**). The detection of LC3 integral optical density (IOD value) in different test groups (**d**). Where in-figure letter, **a** saline group; **b** LPS group; **c** LPS + visfatin group; **d** IOD value graph. $^{*}P < 0.05$, $^{**}P < 0.01$

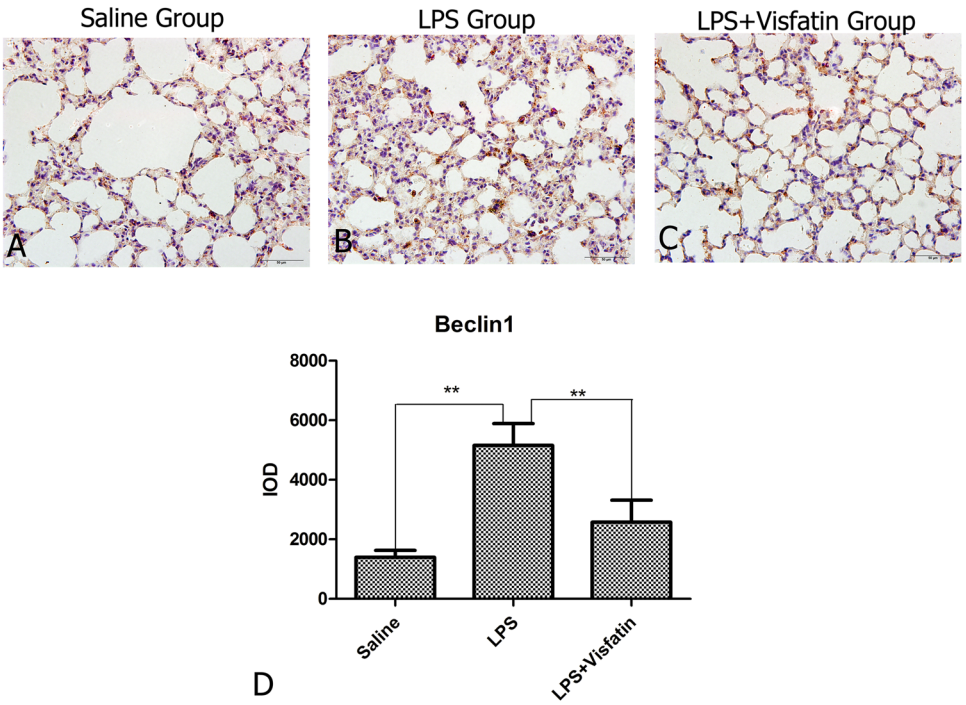

Fig. 8 The distribution pattern of Beclin1 expression in different groups of lung tissues (immunohistochemistry). Yellowish brown reaction product refers to Beclin1 protein-positive signal distribution (**a**–**c**). The detection of Beclin1 integral optical density (IOD value) in different test groups (**d**). Where in-figure letter, **a** saline group; **b** LPS group; **c** LPS + visfatin group; **d** IOD value graph. $^{*}P < 0.05$, $^{**}P < 0.01$

increased in the LPS group. Compared with LPS group, the mRNA expression of LC3 and Beclin1 was decreased in LPS + visfatin group (Fig. 9a, b).

The results of western blot showed that the protein level of LC3 and Beclin1 in the LPS group was significantly increased compared with the control group. Compared with LPS group, the protein expression of LC3 and Beclin1 in LPS + visfatin group showed a decreasing trend (Fig. 9c, d).

Effects of Visfatin on PI3K–AKT Signaling Pathway

Western blot and ImageJ software were used to detect the protein levels of PI3K, AKT, and p-AKT, and to verify if

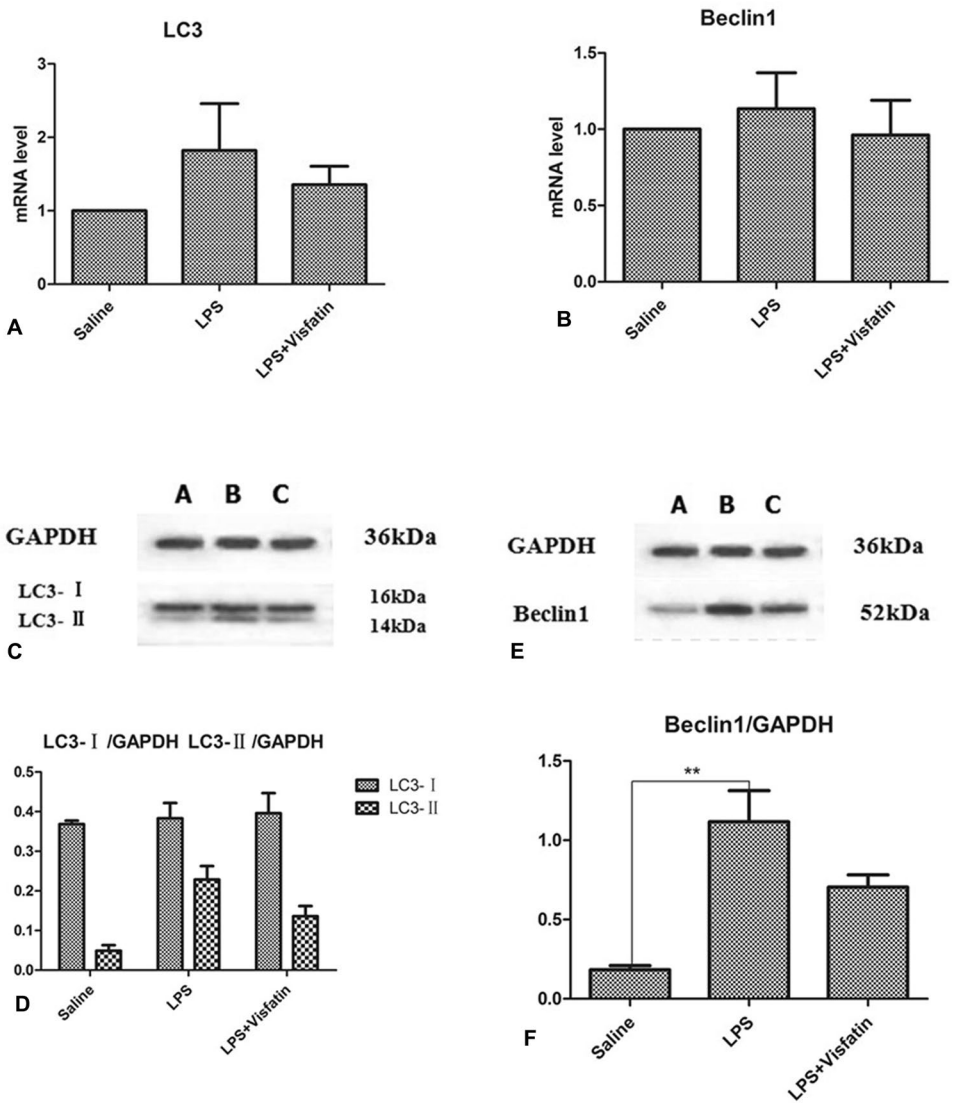

Fig. 9 The mRNA and protein expression changes in LC3 and Beclin1 in different groups of lung tissues. The mRNA expression of LC3 and Beclin1 is shown by qPCR in lung tissue (**a**, **b**). $*P<0.05$, $**P<0.01$. The western blots of LC3, Beclin1 and relative expression of GAPDH along with their gray values (**c**–**f**). Where in-figure letter, A saline group; B LPS group; C LPS + Visfatin group

visfatin was involved in the apoptosis and autophagy by PI3K/AKT signaling pathway in ALI. The results showed that, compared with the control group, the expression of PI3K, AKT and p-AKT was upregulated in the LPS group. Compared with the LPS group, the expression of PI3K and p-AKT was upregulated and the expression of AKT was downregulated in the LPS + visfatin group (Fig. 10a–e).

Discussion

Effect of Visfatin on Lung Tissue Structure of ALI

The current study, for the first time, explored the effects of visfatin on the lung tissue structure in LPS-induced ALI model. The results showed that the ALI model group (LPS group) had considerable lung injury, significantly thickened alveolar walls, and alveolar and lung interstitial hemorrhage and exudation. These symptoms of ALI are consistent with the pathological features including increased lung cell permeability, pulmonary edema, alveolar epithelial cells, and capillary endothelial cell damage mainly described by Moloney and Griffiths (2004). Previously, visfatin showed direct cardioprotective effects by administration of exogenous visfatin (Lim et al. 2008). Compared with LPS group, LPS + visfatin group had thin alveolar septum, slight alveolar congestion, slight pulmonary interstitial and alveoli exudation, and a small amount of inflammatory cell infiltration indicating that visfatin administration caused less degree of lung tissue injury.

VEGF regulates the pulmonary vascular permeability in the lungs (Mura et al. 2004; Pohl-Schickinger et al. 2010). The pulmonary edema and increased vascular permeability are usually implicated in ALI due to exposure of noxious agents (Orfanos et al. 2004). LPS exposure to rats increased the thickness of alveolar wall and caused inflammatory cell

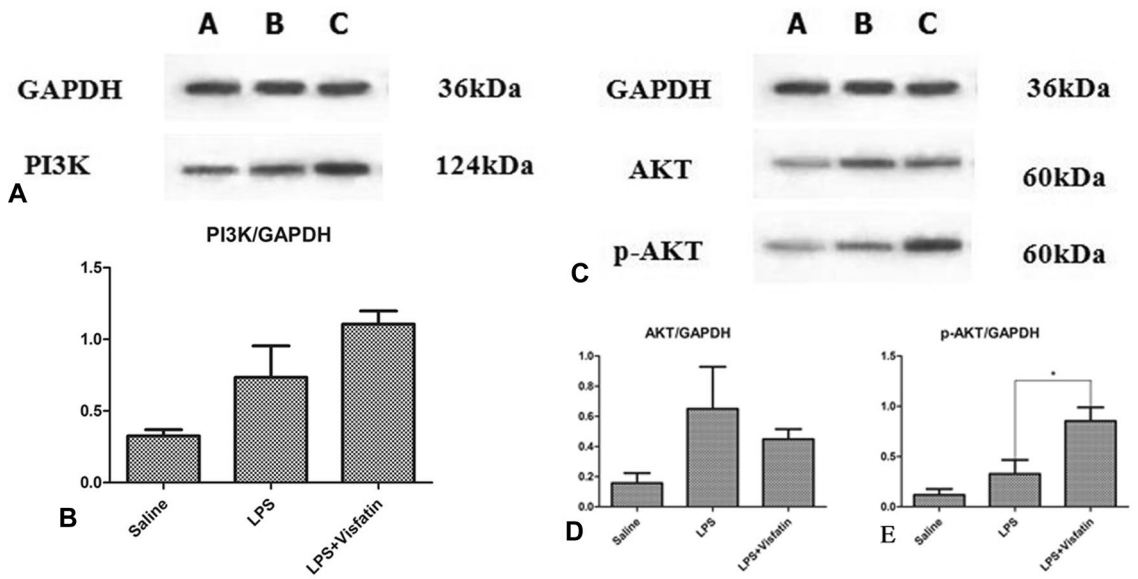

Fig. 10 Western blot analysis of PI3K, AKT and p-AKT in different groups of lung tissues. The western blots of PI3K, AKT, p-AKT and relative expression of GAPDH along with their gray values (**a**–**e**). Where in-figure letter, A saline group; B LPS group; C LPS + visfatin group

infiltration showing ALI lesions in lung tissue sections (Li et al. 2016). Visfatin effectively enhanced the expression of VEGF in human umbilical vein endothelial cells (Adya et al. 2008). In the current study, LPS + visfatin group showed reduced lung tissue VEGF expression than the LPS group indicating that exogenous visfatin inhibits the increase of vascular permeability by reducing the expression of VEGF. Hence, visfatin may alter the cellular permeability by regulating the VEGF expression in lung tissues.

Effect of Visfatin on Apoptosis of Lung Tissue in ALI

During apoptosis, numerous organelles as well as cellular structures are removed by activated caspases (Lockshin and Zakeri 2004). Apoptosis is regulated by genes, and Bcl-2, Bax and Bik (Ashkenazi et al. 2017; Czabotar et al. 2014). The results of qPCR showed that the mRNA expression of Bcl-2 and Bcl-xl in the LPS + visfatin group was significantly higher than that in the LPS group, indicating that LPS-induced ALI promotes apoptosis in the lung tissue, while visfatin can inhibit apoptosis of lung tissue in ALI. This is consistent with the previous findings that visfatin exerts an anti-apoptotic effect on LPS-induced apoptosis of rat splenic lymphocytes, while under immunological stress conditions, visfatin inhibits the apoptosis of rat intestinal mucosal cells and exerts an anti-apoptosis effect (Sitarek et al. 2016; Tacar et al. 2013). The transcription factor, p53, causes apoptosis by cell cycle arrest (at G1 and/or G2 phase) and hampers the cellular growth under stress conditions (Haupt et al. 2003; Jin and Levine 2001). Primarily, p53 acts as a transcription factor, besides it may independently support apoptosis (Moll et al. 2005). Loss of epithelial tissue usually occurs due to dysregulated apoptotic pathways in human ALI (Martin et al. 2003). In the current study, LPS + visfatin group showed lessened lung injury, slight alveolar hyperemia, a little inflammatory cell infiltration in mice lungs and the less number of pulmonary apoptotic cells than the LPS group. In prior studies, visfatin caused inhibition of apoptosis in dose-dependent fashion under bacterial LPS stress (Jia et al. 2004; Sonoli et al. 2011). The protein expression of MLKL was consistent with that of p53, indicating that apoptosis induced by LPS was accompanied by necrotizing apoptosis, and that visfatin could inhibit necrotic apoptosis induced by LPS. This part of the results is also consistent with the detection of results by TUNEL and qPCR methods. Hence, these results indicate that visfatin treatment under LPS stress not only mitigates the histopathological lesions but also inhibits the apoptosis.

Effect of Visfatin on Autophagy of Lung Tissue in ALI

Autophagy is regarded as cell survival-promoting process (Doherty and Baehrecke 2018) or an another type of programmed cell death (Klionsky and Emr 2000) that plays an essential role in sequestering and transporting of cytoplasmic contents via autophagosomes to lysosomes for degradation (Eisenberg-Lerner et al. 2009; Ouyang et al. 2012). The formation of autophagosomes is the key to autophagy (Eskelinen 2008). The results showed that there were few autophagosomes in the saline control group, showing low level of autophagy under physiological conditions (Mizushima et al. 2008). When cells are attacked by pathogenic

factors, mitochondria are damaged (Caroppi et al. 2009; Li et al. 2017). In the current study, the number of autophagy bodies in the LPS group was significantly increased and mitochondria were swollen; our results are in line with the previous findings that pathogenic factors may activate the autophagy or cell survival mechanism (Doherty and Baehrecke 2018). Compared with the LPS group, the number of autophagosomes and mitochondrial damage had significantly reduced in LPS + visfatin group, indicating that exogenous visfatin administration can reduce the level of autophagy and mitochondrial damage in lung injury in the current study. Beclin1 is a homologue of yeast Atg6 and a mammal-specific gene involved in autophagy (Meijer and Codogno 2004). Beclin1 can phosphorylate phosphatidylinositol to form PI3P (Itakura and Mizushima 2009; Mizushima et al. 2011). Microtubule-associated protein 1 LC3 is a homologue of yeast Atg8 gene in mammalian cells and is involved in the formation of autophagosomes (Rzymski et al. 2010; Tanida et al. 2004). The results showed that both LC3 and Beclin1 expressed in the cytoplasm, and most of them were localized in alveolar epithelial and nodular cells. Compared with LPS group, the expression of LC3 and Beclin1 in LPS + visfatin group decreased, indicating that the level of autophagy was decreased after visfatin treatment. These alterations in autophagy expressions are consistent with the observation of autophagosomes under transmission electron microscopy.

The Functional Relationship Between Apoptosis and Autophagy

The functional relationship between autophagy and apoptosis is more complicated (Maiuri et al. 2007). Autophagy and apoptosis are triggered by the displacement of Bcl-2 from Beclin-1 and Bax, respectively, in response to cellular stress (Mukhopadhyay et al. 2014; Pattingre et al. 2005). The inactivation of autophagy factor, Beclin1, increases the number of apoptotic cells (Kang et al. 2011). When Beclin1 binds to the anti-apoptotic protein Bcl-2/Bcl-xL and forms a complex, the function of Beclin1 is inhibited and autophagy cannot be induced (Pattingre and Levine 2006). In this study, the expression of both Beclin1 and the Bcl-2 was increased under LPS stress but decreased following visfatin administration, showing dynamic regulation of autophagy and apoptosis. In addition, apoptosis and autophagy interact at the gene transcription level, and one of the important factors is the p53 (Crighton et al. 2006). p53 is an apoptotic activator that inhibits transcription of the anti-apoptotic factor Bcl-2 (Gao et al. 2011; Levine et al. 2006). In the present study, the expression of p53 is decreased while the expression of Bcl-2 is increased in LPS + visfatin group. When visfatin acts on ALI, p53 expression decreases, Bcl-2 level increases, and autophagic factor (LC3 and beclin 1) expression also decreases, indicating that apoptosis can regulate autophagy. This is consistent with the effect of autophagy on apoptosis (Maiuri et al. 2007), further demonstrating that exogenous visfatin administration inhibits apoptosis and decreases the level of cellular autophagy, thereby promoting the protection of lung tissue.

Effects of Visfatin on PI3K–AKT Signaling Pathway

The activation of PI3K/AKT signaling pathway in ALI can reduce the rate of apoptosis of alveolar type II cells, inhibit the expression of Bax protein, and protect the lung (Bao et al. 2005). Compared with LPS group, the expression of PI3K and p-AKT was upregulated in LPS + visfatin group, indicating the activation of PI3K/AKT signaling pathway in ALI-induced by visfatin. Activated AKT acts on target proteins downstream of the signaling pathway and inhibits apoptosis to promote cell survival (Brunet et al. 1999). The anti-apoptotic mechanism of the PI3K/AKT signaling pathway is related to the Bcl-2 family (Siddiqa et al. 2008). Activated AKT phosphorylates sites on Bad, which in turn binds to its chaperone protein, blocking the binding of Bad to anti-apoptotic proteins (Guo et al. 2011; Henshall et al. 2002). At the same time, activation of the PI3K/AKT signaling pathway can cause phosphorylation of Bax, which inactivates Bax and inhibits apoptosis (Xin and Deng 2005). Therefore, visfatin can activate the PI3K/AKT signaling pathway and by inhibiting the activity of Bcl-2 proteins, inhibits apoptosis in ALI and hence, protects the lung tissues. Moreover, the activation of the PI3K/AKT signaling pathway can upregulate the expression of alveolar epithelial sodium channels in ALI, increase alveolar sodium channels and Na^+–K^+-ATP activity (Qi et al. 2014; Wang et al. 2014). In the LPS-induced ALI model, PI3K/AKT signaling pathway is activated and the content of cAMP in the lung is increased that can reduce the LPS-induced pulmonary microvascular endothelial injury and protect the pulmonary vascular endothelial cells (Guo et al. 2011; Henshall et al. 2002; Reutershan et al. 2010). Therefore, in the present study, following visfatin administration, the degree of pulmonary edema and the expression of VEGF in the lung decreased, indicating that visfatin activates the PI3K/AKT signaling pathway and increases the alveolar sodium channel activity and hence, protects blood vessels of the lung by elevating the levels of cyclic adenosine monophosphate in endothelial cells, which ultimately reduces the degree of lung injury.

Conclusion

1. The visfatin reduces the vascular permeability, the expression of VEGF and the degree of lung injury.

2. The visfatin inhibits apoptosis and reduces the level of autophagy during ALI, demonstrating a cooperative relationship between apoptosis and cell survival mechanism (autophagy).
3. In ALI, visfatin inhibits apoptosis by decreasing the apoptotic rate of alveolar epithelial cells and by regulating the expression of autophagic factors (cell survival mechanism) through activation of PI3K–AKT signaling pathway and hence the level of autophagy is reduced and eventually exerts the protective effect on lung tissue.

Acknowledgements This study was supported by National Natural Science Fund Project of China (no. 31772687) and Fundamental Research Funds for the Central Universities (no. 2662015PY063) and National Natural Science Fund Project of China (no. 31101776).

Compliance with Ethical Standards

Conflict of interest The authors declared no conflict of interests.

References

Adya R, Tan BK, Punn A et al (2008) Visfatin induces human endothelial VEGF and MMP-2/9 production via MAPK and PI3K/Akt signalling pathways: novel insights into visfatin-induced angiogenesis. Cardiovasc Res 78:356–365

Ashkenazi A, Fairbrother WJ, Leverson JD et al (2017) From basic apoptosis discoveries to advanced selective BCL-2 family inhibitors. Nat Rev Drug Discov 16:273–284

Bao S, Wang Y, Sweeney P et al (2005) Keratinocyte growth factor induces Akt kinase activity and inhibits Fas-mediated apoptosis in A549 lung epithelial cells. Am J Physiol Lung Cell Mol Physiol 288:L36–L42

Bi TQ, Che XM (2010) Nampt/PBEF/visfatin and cancer. Cancer Biol Ther 10:119–125

Brunet A, Bonni A, Zigmond MJ et al (1999) Akt promotes cell survival by phosphorylating and inhibiting a Forkhead transcription factor. Cell 96:857–868

Caroppi P, Sinibaldi F, Fiorucci L et al (2009) Apoptosis and human diseases: mitochondrion damage and lethal role of released cytochrome *c* as proapoptotic protein. Curr Med Chem 16:4058–4065

Chen T, Mou Y, Tan J et al (2015) The protective effect of CDDO-Me on lipopolysaccharide-induced acute lung injury in mice. Int Immunopharmacol 25:55–64

Crapo JD (1986) Morphologic changes in pulmonary oxygen toxicity. Annu Rev Physiol 48:721–731

Crighton D, Wilkinson S, O'Prey J et al (2006) DRAM, a p53-induced modulator of autophagy, is critical for apoptosis. Cell 126:121–134

Czabotar PE, Lessene G, Strasser A et al (2014) Control of apoptosis by the BCL-2 protein family: implications for physiology and therapy. Nat Rev Mol Cell Biol 15:49–63

Doherty J, Baehrecke EH (2018) Life, death and autophagy. Nat Cell Biol 20:1110–1117

Eisenberg-Lerner A, Bialik S, Simon HU et al (2009) Life and death partners: apoptosis, autophagy and the cross-talk between them. Cell Death Differ 16:966–975

Emani S, Ramlawi B, Sodha NR et al (2009) Increased vascular permeability after cardiopulmonary bypass in patients with diabetes is associated with increased expression of vascular endothelial growth factor and hepatocyte growth factor. J Thorac Cardiovasc Surg 138:185–191

Erfani S, Aboutaleb N, Oryan S et al (2015) Visfatin inhibits apoptosis and necrosis of hippocampus CA3 cells following transient global ischemia/reperfusion in rats. Int J Pept Res Ther 21:223–228

Eskelinen EL (2008) To be or not to be? Examples of incorrect identification of autophagic compartments in conventional transmission electron microscopy of mammalian cells. Autophagy 4:257–260

Feng X, Jia A (2014) Protective effect of carvacrol on acute lung injury induced by lipopolysaccharide in mice. Inflammation 37:1091–1101

Ferrara N, Gerber H-P, LeCouter J (2003) The biology of VEGF and its receptors. Nat Med 9:669–676

Gao W, Shen Z, Shang L et al (2011) Upregulation of human autophagy-initiation kinase ULK1 by tumor suppressor p53 contributes to DNA-damage-induced cell death. Cell Death Differ 18:1598–1607

Griet M, Zelaya H, Mateos MV et al (2014) Soluble factors from *Lactobacillus reuteri* CRL1098 have anti-inflammatory effects in acute lung injury induced by lipopolysaccharide in mice. PLoS One 9:e110027

Guo Q, Jin J, Yuan JX et al (2011) VEGF, Bcl-2 and Bad regulated by angiopoietin-1 in oleic acid induced acute lung injury. Biochem Biophys Res Commun 413:630–636

Haupt S, Berger M, Goldberg Z et al (2003) Apoptosis—the p53 network. J Cell Sci 116:4077–4085

Henshall DC, Araki T, Schindler CK et al (2002) Activation of Bcl-2-associated death protein and counter-response of Akt within cell populations during seizure-induced neuronal death. J Neurosci 22:8458–8465

Itakura E, Mizushima N (2009) Atg14 and UVRAG: mutually exclusive subunits of mammalian Beclin 1-PI3K complexes. Autophagy 5:534–536

Jia SH, Li Y, Parodo J et al (2004) Pre-B cell colony-enhancing factor inhibits neutrophil apoptosis in experimental inflammation and clinical sepsis. J Clin Investig 113:1318–1327

Jieyu H, Chao T, Mengjun L et al (2012) Nampt/Visfatin/PBEF: a functionally multi-faceted protein with a pivotal role in malignant tumors. Curr Pharm Des 18:6123–6132

Jin S, Levine AJ (2001) The p53 functional circuit. J Cell Sci 114(Pt 23):4139–4140

Kang R, Zeh H, Lotze M et al (2011) The Beclin 1 network regulates autophagy and apoptosis. Cell Death Differ 18:571–580

Ke HL, Lin HH, Li WM et al (2015) High visfatin expression predicts poor prognosis of upper tract urothelial carcinoma patients. Am J Cancer Res 5:2447–2454

Klionsky DJ, Emr SD (2000) Autophagy as a regulated pathway of cellular degradation. Science 290:1717–1721

Levine AJ, Feng Z, Mak TW et al (2006) Coordination and communication between the p53 and IGF-1-AKT-TOR signal transduction pathways. Genes Dev 20:267–275

Li G, Zhou C, Zhou Q et al (2016) Galantamine protects against lipopolysaccharide-induced acute lung injury in rats. Braz J Med Biol Res 49:e5008

Li DX, Hu HY, Li G et al (2017) Calcium controls the formation of vacuoles from mitochondria to regulate microspore development in wheat. Plant Reprod 30:131–139

Lim SY, Davidson SM, Paramanathan AJ et al (2008) The novel adipocytokine visfatin exerts direct cardioprotective effects. J Cell Mol Med 12:1395–1403

Liu F, Sun GQ, Gao HY et al (2013) Angelicin regulates LPS-induced inflammation via inhibiting MAPK/NF-κB pathways. J Surg Res 185:300–309

Lockshin RA, Zakeri Z (2004) Apoptosis, autophagy, and more. Int J Biochem Cell Biol 36:2405–2419
Luk T, Malam Z, Marshall JC (2008) Pre-B cell colony-enhancing factor (PBEF)/visfatin: a novel mediator of innate immunity. J Leukoc Biol 83:804–816
Maiuri MC, Zalckvar E, Kimchi A et al (2007) Self-eating and self-killing: crosstalk between autophagy and apoptosis. Nat Rev Mol Cell Biol 8:741–752
Maloney JP, Ambruso DR, Voelkel NF et al (2014) Platelet vascular endothelial growth factor is a potential mediator of transfusion-related acute lung injury. J Pulm Respir Med 4:212. https://doi.org/10.4172/2161-105X.1000212
Martin TR, Nakamura M, Matute-Bello G (2003) The role of apoptosis in acute lung injury. Crit Care Med 31(4 Suppl):S184–S188
Meijer AJ, Codogno P (2004) Regulation and role of autophagy in mammalian cells. Int J Biochem Cell Biol 36:2445–2462
Mizushima N, Levine B, Cuervo AM et al (2008) Autophagy fights disease through cellular self-digestion. Nature 451:1069–1075
Mizushima N, Yoshimori T, Ohsumi Y (2011) The role of Atg proteins in autophagosome formation. Annu Rev Cell Dev Biol 27:107–132
Moll UM, Wolff S, Speidel D et al (2005) Transcription-independent pro-apoptotic functions of p53. Curr Opin Cell Biol 17:631–636
Moloney ED, Griffiths MJD (2004) Protective ventilation of patients with acute respiratory distress syndrome. Br J Anaesth 92:261–270
Mukhopadhyay S, Panda PK, Sinha N et al (2014) Autophagy and apoptosis: where do they meet? Apoptosis 19:555–566
Mura M, Santos CCd, Stewart D et al (2004) Vascular endothelial growth factor and related molecules in acute lung injury. J Appl Physiol 97:1605–1617
Okuda S, Sherman DJ, Silhavy TJ et al (2016) Lipopolysaccharide transport and assembly at the outer membrane: the PEZ model. Nat Rev Microbiol 14:337–345
Orfanos SE, Mavrommati I, Korovesi I et al (2004) Pulmonary endothelium in acute lung injury: from basic science to the critically ill. Intensive Care Med 30:1702–1714
Ouyang L, Shi Z, Zhao S et al (2012) Programmed cell death pathways in cancer: a review of apoptosis, autophagy and programmed necrosis. Cell Prolif 45:487–498
Parekh D, Dancer RC, Thickett DR (2011) Acute lung injury. Clin Med 11:615–618
Pattingre S, Levine B (2006) Bcl-2 inhibition of autophagy: a new route to cancer? Cancer Res 66:2885–2888
Pattingre S, Tassa A, Qu X et al (2005) Bcl-2 antiapoptotic proteins inhibit Beclin 1-dependent autophagy. Cell 122:927–939
Pohl-Schickinger A, Koehne P, Schmitz T et al (2010) Vascular endothelial growth factor and its soluble receptor in infants with congenital cardiac disease. Cardiol Young 20:505–508
Qi D, He J, Wang D et al (2014) 17β-estradiol suppresses lipopolysaccharide-induced acute lung injury through PI3K/Akt/SGK1 mediated up-regulation of epithelial sodium channel (ENaC) in vivo and in vitro. Respir Res 15:159
Reddy NM, Suryanaraya V, Yates MS et al (2009) The triterpenoid CDDO-imidazolide confers potent protection against hyperoxic acute lung injury in mice. Am J Respir Crit Care Med 180:867–874
Reutershan J, Saprito MS, Wu D et al (2010) Phosphoinositide 3-kinase γ required for lipopolysaccharide-induced transepithelial neutrophil trafficking in the lung. Eur Respir J 35:1137–1147
Rzymski T, Milani M, Pike L et al (2010) Regulation of autophagy by ATF4 in response to severe hypoxia. Oncogene 29:4424–4435
Schwechheimer C, Kuehn MJ (2015) Outer-membrane vesicles from Gram-negative bacteria: biogenesis and functions. Nat Rev Microbiol 13:605–619
Siddiqa A, Long LM, Li L et al (2008) Expression of HER-2 in MCF-7 breast cancer cells modulates anti-apoptotic proteins Survivin and Bcl-2 via the extracellular signal-related kinase (ERK) and phosphoinositide-3 kinase (PI3K) signalling pathways. BMC Cancer 8:129
Sitarek P, Skała E, Toma M et al (2016) A preliminary study of apoptosis induction in glioma cells via alteration of the Bax/Bcl-2-p53 axis by transformed and non-transformed root extracts of *Leonurus sibiricus* L. Tumor Biol 37:8753–8764
Sonoli S, Shivprasad S, Prasad C et al (2011) Visfatin—a review. Eur Rev Med Pharmacol Sci 15:9–14
Sun Z, Lei H, Zhang Z (2013) Pre-B cell colony enhancing factor (PBEF), a cytokine with multiple physiological functions. Cytokine Growth Factor Rev 24:433–442
Tacar O, Sriamornsak P, Dass CR (2013) Doxorubicin: an update on anticancer molecular action, toxicity and novel drug delivery systems. J Pharm Pharmacol 65:157–170
Tanida I, Ueno T, Kominami E (2004) LC3 conjugation system in mammalian autophagy. Int J Biochem Cell Biol 36:2503–2518
Wang Q, Zheng X, Cheng Y et al (2014) Resolvin D1 stimulates alveolar fluid clearance through alveolar epithelial sodium channel, Na, K-ATPase via ALX/cAMP/PI3K pathway in lipopolysaccharide-induced acute lung injury. J Immunol 192:3765–3777
Wu XT, Yang Z, Ansari AR et al (2018) Visfatin regulates the production of lipopolysaccharide-induced inflammatory cytokines through p38 signaling in murine macrophages. Microb Pathog 117:55–59
Xiao K, Zou WH, Yang Z et al (2015) The role of visfatin on the regulation of inflammation and apoptosis in the spleen of LPS-treated rats. Cell Tissue Res 359:605–618
Xin M, Deng X (2005) Nicotine inactivation of the proapoptotic function of Bax through phosphorylation. J Biol Chem 280:10781–10789
Yang W, Zeng Y, Li B et al (2015) Pre-B-cell colony enhancing factor (PBEF) increases endothelial permeability in hypoxia/re-oxygenation model. Int J Clin Exp Med 8:8842–8847
Yen YT, Yang HR, Lo HC et al (2013) Enhancing autophagy with activated protein C and rapamycin protects against sepsis-induced acute lung injury. Surgery 153:689–698
Zhou Y, Yuan HR, Cui L et al (2017) Effects of visfatin on the apoptosis of intestinal mucosal cells in immunological stressed rats. Acta Histochem 119:26–31